Effects of Relative Instrument Orientation upon Gravity Gradiometer System Performance

Eugene J. Pelka*
Lockheed Missiles and Space Company, Sunnyvale, Calif.
and
Daniel B. DeBra†
Stanford University, Stanford, Calif.

There are three moving-base gravity gradiometers currently being developed. Two of these instruments are spinners and produce gradient measurements at twice their spin frequency. The third is a torsion balance instrument and measures components of the gradient tensor at zero frequency. A system of at least three sensors of any one type is required to measure completely the gravity gradient. This paper defines the optimal relative orientations of the sensors which comprise a gradient measurement system. Three- and four-sensor systems are considered. The theory of conservative fields and their gradient is reviewed briefly. The three different gradiometers are described.

I. Introduction

A GRAVITY gradiometer measures the spatial gradient of the gravity field in which it operates. Substantial interest in these instruments has arisen in recent years, with suggested applications ranging from missile and aircraft guidance[1,2] to oil well exploration.[3] The first gradiometers (Eötvös, 1880) were fixed-base instruments, requiring up to 30 min to provide a single measurement. The new moving-base gradiometers will be mounted in aircraft, ships, or even jeeps and will provide a gradient measurement in approximately 10 s.

There are three moving-base gravity gradiometers currently under development. The instruments are being developed at the Hughes Research Laboratories,[4] the Bell Aerospace Corporation,[5] and the Charles Stark Draper Laboratory.[6,7] The design goal for each of the sensors is 1 Eötvös unit (1 EU is 10^{-9} s^{-2}). Two of the sensors were designed specifically to measure the gravity gradient. The third uses existing accelerometers to provide a gradient measurement. The Hughes and Bell instruments rotate, modulating the information. This rotation transfers the gravity gradient signal to a higher frequency, quieter portion of the spectrum and separates the signal from some sources of instrument bias. The Draper Laboratory sensor measures the gradient at zero frequency and uses a sophisticated floatation suspension system to isolate the sensing element from errors induced by rotation and jitter.

A system of at least three instruments of any one type is required to measure gravity gradient tensor. The primary objective of this paper is to define the optimal relative orientations of the three sensors which comprise a minimum gravity gradient measurement system. In addition, the effects are considered of different relative sensor orientations when a fourth, redundant sensor is included.

II. Gravity Field and Its Gradient

A gravity field is conservative and may be expressed as a scalar function φ of position $\vec{r}$ relative to the attracting body. At any point $\vec{r}$, the gravitational acceleration $\vec{g}$ due to that body is

$$\vec{g} = \nabla\varphi(\vec{r}) \tag{1}$$

Expressing $\vec{g}$ in a set of Cartesian coordinates, Eq. (1) becomes

$$[\vec{g}]^T = \left[\frac{\partial\varphi}{\partial x}, \frac{\partial\varphi}{\partial y}, \frac{\partial\varphi}{\partial z}\right] \tag{2}$$

The spatial gradient of the gravity vector $\vec{g}$ is the second-order tensor of Eq. (3):

$$[\nabla\vec{g}] = \begin{bmatrix} \frac{\partial^2\varphi}{\partial x^2} & \frac{\partial^2\varphi}{\partial x\partial y} & \frac{\partial^2\varphi}{\partial x\partial z} \\ \frac{\partial^2\varphi}{\partial y\partial x} & \frac{\partial^2\varphi}{\partial y^2} & \frac{\partial^2\varphi}{\partial y\partial z} \\ \frac{\partial^2\varphi}{\partial z\partial x} & \frac{\partial^2\varphi}{\partial z\partial y} & \frac{\partial^2\varphi}{\partial z^2} \end{bmatrix} \tag{3}$$

To determine completely the gravity gradient tensor, all of the independent components must be measured. For a conservative gravitation force,[8]

$$\nabla\times\vec{g} = 0 \tag{4}$$

$$\nabla\cdot\vec{g} = 0 \tag{5}$$

Equation (4) expresses the symmetry of the gradient tensor. Equation (5) is Laplace's equation and requires that the sum of the diagonal components of the gradient tensor be zero. Since the gradient tensor is symmetric, no more than six of its nine components are independent. The scalar Laplace equation reduces the total number of independent elements to five. Therefore, complete determination of the gravity gradient tensor at any point in space requires only five independent measurements.

To follow convention, the gradient tensor will be represented by $\vec{\Gamma}$:

$$[\vec{\Gamma}] \triangleq \begin{bmatrix} \Gamma_{xx} & \Gamma_{xy} & \Gamma_{xz} \\ \Gamma_{xy} & \Gamma_{yy} & \Gamma_{yz} \\ \Gamma_{xz} & \Gamma_{yz} & \Gamma_{zz} \end{bmatrix} \tag{6}$$

Presented as Paper 77-1070 at the AIAA 1977 Guidance and Control Conference, Hollywood, Fla., Aug. 8-10, 1977; submitted Oct. 3, 1977; revision received May 22, 1978.

Index category: Sensor Systems.

*Engineer. Member AIAA.
†Professor of Aeronautics and Astronautics, Guidance and Control Laboratory. Fellow AIAA.

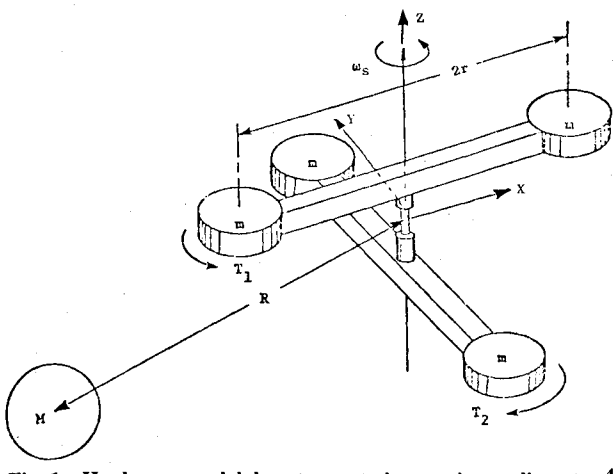

Fig. 1 Hughes research laboratory rotating gravity gradiometer.[4]

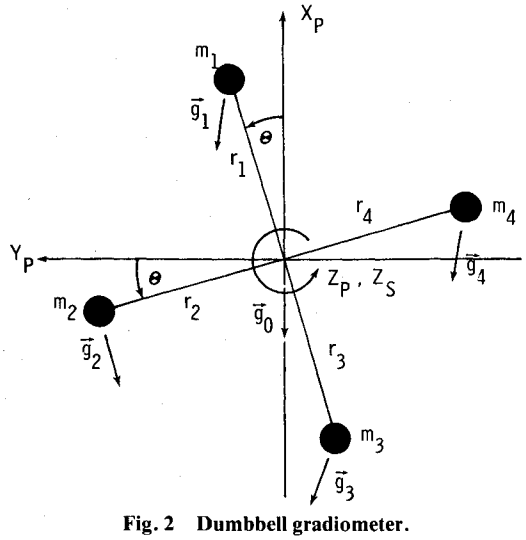

Fig. 2 Dumbbell gradiometer.

III. Hughes' Rotating Gravity Gradiometer

The Hughes' rotating gravity gradiometer measures gravity gradient at a nonzero frequency. The instrument, shown in Fig. 1, can be thought of as two identical arms connected by a flex pivot. The relative torque acting upon the arms is sensed by a piezoelectric transducer as the pivot is strained. The gravity gradient signal excites a lightly damped differential rotation mode at twice the 17.5-Hz spin frequency. The sensor is tuned to have a resonance at 35 Hz.

Consider the ideal dumbell gradiometer oriented with its spin axis $\hat{z}_s$ horizontal, as shown in Fig. 2. The vector $\vec{g}_0$ is the gravity vector at the orgin of the sensor (subscript s) axis reference system and defines the local horizontal plane.

At any of the masses, m_1, for example, the gravity vector to first order can be written in terms of g_0 as in

$$g_{1_j} = g_{0_j} + \frac{\partial g_j}{\partial k}\Delta k: \qquad j=x,y,z; \qquad k=x,y,z \tag{7}$$

Using Eq. (6) and the definition

$$\vec{\Delta r} \triangleq (\Delta x, \Delta y, \Delta z)^T \tag{8}$$

the gravity at m_1 may be written as

$$\vec{g}_1 = \vec{g}_0 + \vec{\Gamma}\cdot\vec{\Delta r}_1 \tag{9}$$

Since $\vec{\Delta r}_1$ refers to the displacement of m_1 from the origin of the sensor reference system,

$$\vec{\Delta r}_1 \equiv \vec{r}_1 \tag{10}$$

and Eq. (9) may be written as

$$\vec{g}_1 = \vec{g}_0 + \vec{\Gamma}\cdot\vec{r}_1 \tag{11}$$

The torque $\vec{T}_o$ induced by the gravitational field influence upon the odd arm may be written as

$$\vec{T}_o = \vec{r}_1 \times \vec{f}_1 + \vec{r}_3 \times \vec{f}_3 \tag{12}$$

where

$$\vec{f}_1 = m_1\{\vec{g}_0 + \vec{\Gamma}\cdot\vec{r}_1\} \tag{13}$$

$$\vec{f}_3 = m_3\{\vec{g}_0 + \vec{\Gamma}\cdot\vec{r}_3\} \tag{14}$$

Since for an ideal instrument all four masses m_1 are equal, and since

$$\vec{r}_3 = -\vec{r}_1 \tag{15}$$

then Eq. (12) can be rewritten as

$$\vec{T}_o = 2m\vec{r}_1 \times \{\vec{\Gamma}\cdot\vec{r}_1\} \tag{16}$$

An equation similar to Eq. (16) can be written for even arm induced torques, and therefore the differential output torque induced by the gravity gradient is

$$\vec{T}_o - \vec{T}_e = 2m\{[\vec{r}_1 \times \vec{\Gamma}\cdot\vec{r}_1] - [\vec{r}_2 \times \vec{\Gamma}\,\vec{r}_2]\} \tag{17}$$

Along the sensitive axis $\hat{z}_s$, the component of the differential torque vector of Eq. (17) is

$$(\vec{T}_o - \vec{T}_e)\cdot\hat{z}_s = 2mr^2\{2(\Gamma_{yy} - \Gamma_{xx})\sin\theta\cos\theta + 2\Gamma_{xy}(\cos^2\theta - \sin^2\theta)\} \tag{18}$$

or

$$(\vec{T}_o - \vec{T}_e)\cdot\hat{z}_s = 2mr^2\{(\Gamma_{yy} - \Gamma_{xx})\sin 2\theta + 2\Gamma_{xy}\cos 2\theta\} \tag{19}$$

By separating the in-phase ($\sin 2\theta$) and quadrature ($\cos 2\theta$) components of output Eq. (19), measurements containing three of the five independent terms of the gravity gradient tensor are available.

IV. Bell Aerospace Corporation Gradiometer

The sensitive elements of the Bell Aerospace gravity gradiometer are four modified Bell model VII pendulous accelerometers. The accelerometers are mounted symmetrically on a spin table with their sensitive axes in the tangential direction defined by $\hat{s}$, where

$$\hat{s} = \hat{\omega} \times \hat{r} \tag{20}$$

The nominal spin table rate is 0.5 Hz. A conceptual diagram of the Bell instrument is shown in Fig. 3. The instrument senses gravity gradient in the X-Y plane according to the equation

$$[(a_1 + a_2) - (a_3 + a_4)] = 2r\{(\Gamma_{yy} - \Gamma_{xx})\sin(2\omega t) + 2\Gamma_{xy}\cos(2\omega t)\} \tag{21}$$

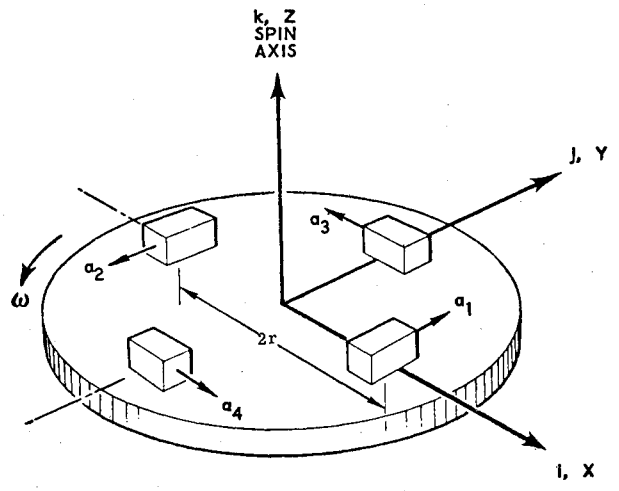

Fig. 3 Bell Aerospace heavy proof mass accelerometer gradiometer.

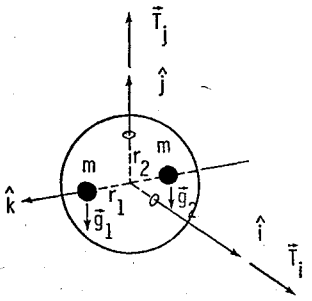

Fig. 4 Simplified representation of Draper Laboratory spherical gravity gradiometer; output axes $\hat{i}$ and $\hat{j}$.

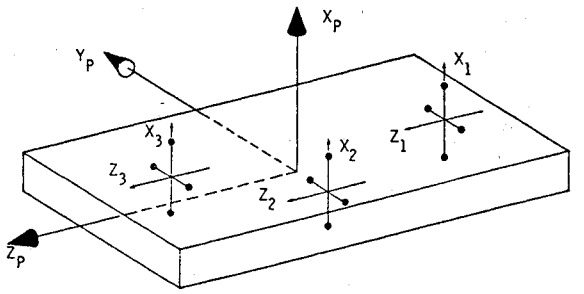

Fig. 5 Hughes' sensor system initial orientation for purposes of spin axis alignment specification.

Modulation of the output signal yields an in-phase measurement of the off-diagonal gravity gradient tensor component Γ_{xy} and a quadrature measurement of the difference between two of the diagonal terms $\Gamma_{xx}-\Gamma_{yy}$. Comparison of Eqs. (19) and (21) shows that the output equations for both of the rotating gravity gradiometers are equivalent.

V. Draper Laboratory Gravity Gradiometer

The Draper Laboratory instrument senses the gravity gradient signal at zero frequency; i.e., the instrument does not rotate. A conceptual drawing of the Draper Laboratory spherical gradiometer is shown in Fig. 4. The spherical gradiometer uses a spherical float having dense masses attached at two points, which provide a dumbell mass distribution, as shown in the figure. External torques are sensed about each of the two perpendicular axes (i, j) which define a plane normal to the between-the-weights axis (k). The flotation fluid is inviscid, providing a degree of isolation from small-amplitude (jitter) rotations of the case. The output vector equation for the spherical gradiometer is

$$[\vec{T}_g] = 2mr^2\,[-\Gamma_{yz}, \Gamma_{xz}, 0]^T \tag{22}$$

VI. Measuring the Gravity Gradient with Rotating Gravity Gradiometers‡

A directional reference frame for three rotating gravity gradiometers is shown in Fig. 5. We assume that the sensors are not spinning and that the sensor axes (x_j, y_j, z_j) are, respectively, coincident with platform axes (x_p, y_p, z_p). The separate sensor reference system orientations then can be varied arbitrarily using a {1, 2, 3} Euler rotation sequence defined by angles $\{\alpha_j, \beta_j, \gamma_y\}$. Subsequent to these alignment rotations, the sensors are spun up and measurements taken. The output of each sensor corresponds to Eq. (19), with each sensor measuring components of the gravity gradient tensor expressed relative to the newly specified body (sensor) reference directions. In order for these measurements to provide a complete estimate of the gravity gradient tensor, all six outputs from the three sensors must be related to a single reference frame. For convenience, this frame has been defined to be the platform reference frame. It is easy to show that

$$\vec{\Gamma}_B = T_{B/P}\vec{\Gamma}_P T^T_{B/P} \tag{23}$$

Sensor in-phase and quadrature signals are averaged over a 10-s sample period to provide measurements of $[\Gamma_{yy}-\Gamma_{xx}]_{Bj}$ and $[\Gamma_{xy}]_{Bj}$ as specified by

$$[A_{IP}]_j = 4mr^2\,[\tfrac{1}{2}(\Gamma_{yy}-\Gamma_{xx})]_{Bj} \tag{24}$$

$$[A_Q]_j = 4mr^2\,[\Gamma_{xy}]_{Bj} \tag{25}$$

Using Eq. (23), the right sides of Eqs. (24) and (25) can be expressed in terms of the platform referenced gradient tensor for arbitrary Euler angle rotations $\{\alpha, \beta, \gamma\}_j$. Equations (24) and (25) can be rewritten for all three sensors in terms of the platform-referenced gradient tensor as

$$\frac{1}{4mr^2}\begin{bmatrix} A_{IP} \\ A_Q \end{bmatrix}_j = \begin{bmatrix} -\tfrac{1}{2}c^3_{\beta_j}c_{2\gamma_j} & \tfrac{1}{2}c_{2\gamma_j}(c^2_{\alpha_j}-s^2_{\alpha_j}s^2_{\beta_j}) & \tfrac{1}{2}c_{2\gamma_j}(s^2_{\alpha_j}-c^2_{\alpha_j}s^2_{\beta_j}) & -\tfrac{1}{2}c_{2\gamma_j}s_{2\beta_j}s_{\alpha_j} & \tfrac{1}{2}c_{2\gamma_j}s_{2\beta_j}c_{\alpha_j} & \tfrac{1}{2}c_{2\gamma_j}s_{2\alpha_j}(1+s^2_{\beta_j}) \\ & -\tfrac{1}{2}s_{2\gamma_j}s_{2\alpha_j}s_{\beta_j} & -\tfrac{1}{2}s_{2\gamma_j}s_{2\alpha_j}s_{\beta_j} & -\tfrac{1}{2}s_{2\gamma_j}c_{\beta_j}s_{\alpha_j} & -\tfrac{1}{2}s_{2\gamma_j}c_{\beta_j}s_{\alpha_j} & +c_{2\alpha_j}s_{2\gamma_j} \\ & \tfrac{1}{2}s_{2\gamma_j}(c^2_{\gamma_j}-s^2_{\beta_j}s^2_{\alpha_j}) & \tfrac{1}{2}s_{2\gamma_j}(s^2_{\gamma_j}-c^2_{\alpha_j}s^2_{\beta_j}) & c_{2\gamma_j}c_{\beta_j}c_{\alpha_j} & c_{2\gamma_j}c_{\beta_j}s_{\alpha_j} & \tfrac{1}{2}s_{2\gamma_j}s_{2\alpha_j}(1+s^2_{\beta_j}) \\ -\tfrac{1}{2}s_{2\gamma_j}c^2_{\beta_j} & +\tfrac{1}{2}c_{2\gamma_j}s_{\beta_j}s_{2\alpha_j} & -\tfrac{1}{2}c_{2\gamma_j}s_{2\alpha_j}s_{\beta_j} & -\tfrac{1}{2}s_{2\gamma_j}s_{2\beta_j}s_{\alpha_j} & +\tfrac{1}{2}s_{2\gamma_j}s_{2\beta_j}c_{\alpha_j} & +s_{\beta_j}(c_{2\gamma_j}s^2_{\alpha_j}-c_{2\alpha_j}c^2_{\gamma_j}) \end{bmatrix} \begin{bmatrix} \Gamma_{xx} \\ \Gamma_{yy} \\ \Gamma_{zz} \\ \Gamma_{xy} \\ \Gamma_{xz} \\ \Gamma_{yz} \end{bmatrix}_{j=1,2,3} \tag{26}$$

$$(1/4mr^2)\,[A_j] = [M']\,[\vec{\Gamma}] \tag{27}$$

‡Since the signal equations are the same for both the Hughes and Bell sensors, it is understood that the analysis of signal estimation for the Hughes' sensor applies directly to the Bell Sensor also.

The six different elements of the gradient tensor $\vec{\vec{\Gamma}}$ appear as the vector $\vec{\Gamma}$ in output Eqs. (26) and (27). The order of the six elements of the vector is defined by Eq. (26). In subsequent discussions, the estimate of $\vec{\Gamma}$ will be denoted by $\hat{\Gamma}$. The error in the estimate of $\vec{\Gamma}$ will be denoted by $\tilde{\Gamma}$.

The 6×6 matrix M' of Eqs. (26) and (27) is singular due to the Laplace relationship of Γ_{xx}, Γ_{yy}, Γ_{zz}, as shown in Eq. (5). We can remove the effect of this singularity either by eliminating one of the gradient tensor principal diagonal terms [using Eq. (5)] or by adding the Laplace equation to Eq. (26) as a seventh measurement having zero error. The addition of Laplace's equation as a measurement allows all of the terms of the gradient tensor to be treated in the same way mathematically. Combination of Eq. (5) with Eq. (27) yields

$$\frac{1}{4mr^2}\begin{bmatrix} A'_{6\times1} \\ \hline 0 \end{bmatrix} = \left[\begin{array}{c} M'_{6\times6} \\ \hline 1\ 1\ 1\ 0\ 0\ 0 \end{array}\right][\vec{\Gamma}] \tag{28}$$

or

$$[A] = [M]_{7\times6}[\vec{\Gamma}] \tag{29}$$

With

$$[B] \triangleq [M^T M]^{-1}[M^T] \tag{30}$$

the least-squares error solution estimate of $[\vec{\Gamma}]$ is

$$[\hat{\Gamma}] = BA_M \tag{31}$$

where

$$A_M \triangleq A + V \tag{32}$$

Matrix V is a 7×1 vector representing measurement noise. The first six terms of vector V are taken to be white, zero mean Gaussian random variables having variance 1 $(EU)^2$. The seventh component, V_7, is exactly zero. Furthermore,

$$\mathcal{E}(V\ V^T) = \left[\begin{array}{c|c} I_{6\times6} & \\ \hline O_{1\times6} & O_{7\times1} \end{array}\right] \tag{33}$$

Equation (33) states that the six actual measurements have uncorrelated errors of variance 1 EU^2. With

$$\tilde{\Gamma} \triangleq \hat{\Gamma} - \vec{\Gamma} \tag{34}$$

and

$$P_{6\times6} \triangleq \mathcal{E}[\tilde{\Gamma}\tilde{\Gamma}^T] \tag{35}$$

then

$$P = B\ \ R\ \ B^T \tag{36}$$

where

$$R \triangleq \mathcal{E}[V\ \ V^T] \tag{37}$$

The reciprocal of this matrix, R, would be used to obtain a matrix B [see Eq. (30)] for the weighted least-squares solution. However, the singularity produced by the perfect measurement from Laplace's equation requires special handling of R. We have chosen to use the simple least-squares solution because we conjecture that the relative orientation (α, β, γ) will be the same for both solutions, since Laplace's equation is a constraint on magnitudes.

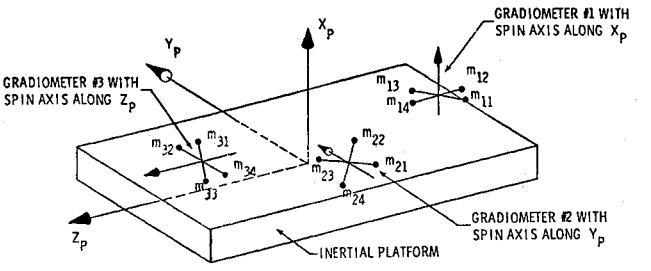

Fig. 6 Baseline Hughes' gradiometer gradient measuring system.

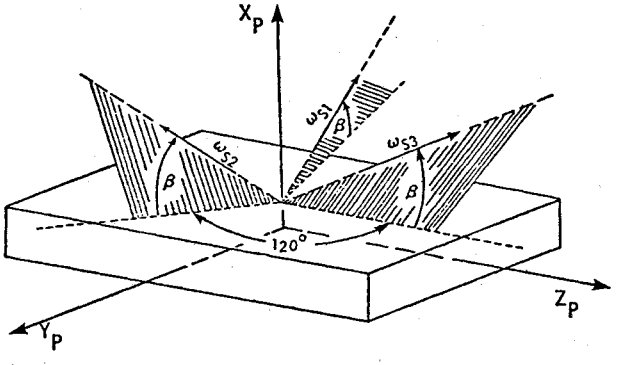

Fig. 7 Closing the spin axis umbrella on $\hat{x}_p$.

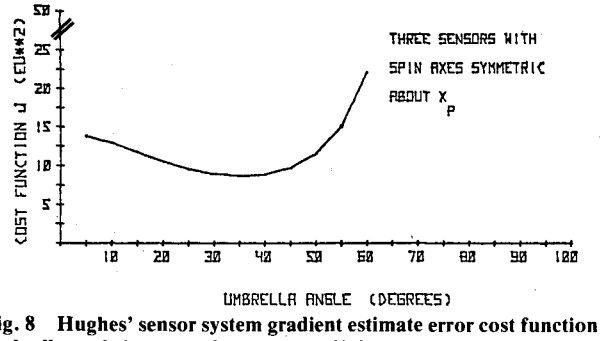

Fig. 8 Hughes' sensor system gradient estimate error cost function as umbrella angle increases from zero to 60 deg.

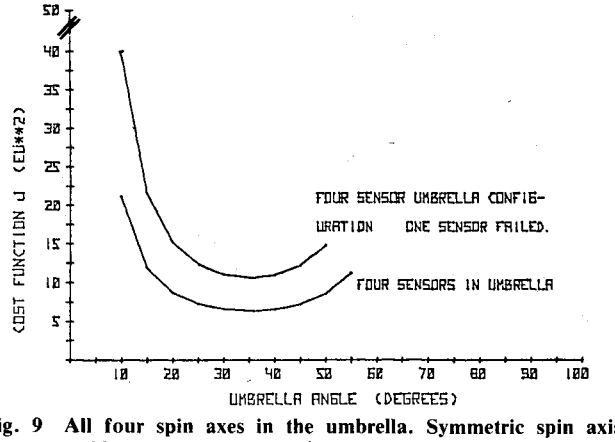

Fig. 9 All four spin axes in the umbrella. Symmetric spin axis placement (90-deg intervals) about $\hat{x}_p$.

Given Eq. (36), the problem is to find angles $(\alpha,\beta,\gamma)_j$ (which determine B) so that a scalar cost function J, which is dependent upon covariance matrix P, is minimized. The purpose of this analysis is to determine the relative sensor orientations that minimize the error in the estimate of the gravity gradient. If the error model considered is to be independent of the actual gradient tensor, it also should be independent of the coordinate frame into which the gradient estimates are resolved. The cost function of Eq. (38)

(suggested by John V. Breakwell) meets these criteria:

$$J=\mathrm{Tr}\{\mathcal{E}[\tilde{\vec{\Gamma}}\tilde{\vec{\Gamma}}^T]\} \tag{38}$$

$\tilde{\vec{\Gamma}}$ is defined by the 3×3 matrix composed of the errors in the estimate of $\vec{\Gamma}$. With $\tilde{\Gamma}$ defined by Eq. (34),

$$\tilde{\vec{\Gamma}}=\begin{bmatrix}\tilde{\Gamma}_1 & \tilde{\Gamma}_4 & \tilde{\Gamma}_5\\ \tilde{\Gamma}_4 & \tilde{\Gamma}_2 & \tilde{\Gamma}_6\\ \tilde{\Gamma}_5 & \tilde{\Gamma}_6 & \tilde{\Gamma}_3\end{bmatrix} \tag{39}$$

$$\mathcal{E}[\tilde{\vec{\Gamma}}\tilde{\vec{\Gamma}}^T]=\mathcal{E}\begin{bmatrix}\tilde{\Gamma}_1^2+\tilde{\Gamma}_4^2+\tilde{\Gamma}_5^2 & \tilde{\Gamma}_1\tilde{\Gamma}_4+\tilde{\Gamma}_4\tilde{\Gamma}_1+\tilde{\Gamma}_5\tilde{\Gamma}_6 & \tilde{\Gamma}_1\tilde{\Gamma}_5+\tilde{\Gamma}_4\tilde{\Gamma}_6+\tilde{\Gamma}_5\tilde{\Gamma}_3\\ & \tilde{\Gamma}_4^2+\tilde{\Gamma}_2^2+\tilde{\Gamma}_6^2 & \tilde{\Gamma}_4\tilde{\Gamma}_5+\tilde{\Gamma}_2\tilde{\Gamma}_6+\tilde{\Gamma}_6\tilde{\Gamma}_3\\ & & \tilde{\Gamma}_5^2+\tilde{\Gamma}_6^2+\tilde{\Gamma}_3^2\end{bmatrix} \tag{40}$$

$$\mathrm{Tr}\mathcal{E}[\tilde{\vec{\Gamma}}\tilde{\vec{\Gamma}}^T]=\tilde{\Gamma}_{xx}^2\tilde{\Gamma}_{yy}+\tilde{\Gamma}_{zz}^2+2[\tilde{\Gamma}_{xy}^2+\tilde{\Gamma}_{xz}^2+\tilde{\Gamma}_{zy}^2] \tag{41}$$

If T transforms the measure numbers of a vector expressed on an orthonormal basis A to those in basis B, then $\vec{\Gamma}$ transforms by the similarity transformation

$$\vec{\Gamma}_A=T\vec{\Gamma}_B T^T \tag{42}$$

Using Eq. (42),

$$\tilde{\vec{\Gamma}}_A=T\tilde{\vec{\Gamma}}_B T^T \tag{43}$$

Hence,

$$\tilde{\vec{\Gamma}}_A\tilde{\vec{\Gamma}}_A^T=T\tilde{\vec{\Gamma}}_B T^T T\tilde{\vec{\Gamma}}_B^T T^T \tag{44}$$

and, since the the trace is invariant under similarity transformation,

$$\mathrm{Tr}\{\mathcal{E}[\tilde{\vec{\Gamma}}_A\tilde{\vec{\Gamma}}_A^T]\}=\mathrm{Tr}\{\mathcal{E}[\tilde{\vec{\Gamma}}_B\tilde{\vec{\Gamma}}_B^T]\} \tag{45}$$

This invariance allows the cost function to provide a scalar measure of the quality of the gradient estimate without regard for the coordinate system to which the measurements are referenced.

The system shown in Fig. 6 is taken as the baseline gradient measurement case. The spin axis of each sensor is parallel to a different platform reference direction. For this sensor system orientation, J had the value 8.667 EU^2. The Euler angles corresponding to this set of sensor orientations are

$$\begin{bmatrix}\alpha_1 & \beta_1 & \gamma_1\\ \alpha_2 & \beta_2 & \gamma_2\\ \beta_3 & \beta_3 & \gamma_3\end{bmatrix}=\begin{bmatrix}0 & 90 & 0\\ 270 & 0 & 0\\ 0 & 0 & 0\end{bmatrix}\ \text{deg} \tag{46}$$

This particular set of sensor spin axis orientations minimized J for all sets of sensor spin axis directions considered.

A test of the Hughes' sensor system gravity gradient estimation for the case where the spin axes were not orthogonal is shown in Fig. 7. This test was initialized by symmetrically placing the three sensor spin axes about $\hat{x}_p$ in the $\hat{y}_p$-$\hat{z}_p$ plane. The sensor spin axes then were rotated uniformly out of the $\hat{y}_p$-$\hat{z}_p$ plane toward $\hat{x}_p$ through an increasing angle β in a manner similar to closing an umbrella. The results of this test are given in Fig. 8. As the umbrella angle increased from 5 to 35 deg, the cost function decreased from 13.9 EU^2 to its minimum value of 8.667 EU^2 at 35.26 deg. At that angle, the spin axes were orthogonal. As the umbrella continued to close, the cost function again began to increase, principally due to a loss in the accuracy of the Γ_{xx} estimate.

The cost function analysis was extended to include four instruments. A fourth instrument provides protection against loss of mission due to the failure of a single gradiometer. Several four-instrument operating configurations were considered:

1) All four spin axes were placed symmetrically about $\hat{x}_p$ in the $\hat{y}_p$-$\hat{z}_p$ plane. The umbrella was closed with all four spin axes collapsing toward $\hat{x}_p$.

2) One spin axis was oriented along $\hat{x}_p$. The three other spin axes were placed symmetrically about $\hat{x}_p$ in the $\hat{y}_p$-$\hat{z}_p$ plane. The umbrella was closed as in Fig. 7.

The results of these tests appear in Figs. 9 and 10. Figure 9 shows that, for the sensor configuration defined by case 1, an umbrella angle of 35 deg is optimal for both the four-sensor case and the case of one instrument failed. For the full four-sensor case, the cost function has minimum value of 6.4 EU^2. With one sensor failed, this value increased to 10.6 EU^2.

The results of aligning one sensor spin axis along $\hat{x}_p$ and the three others in an umbrella are given in Fig. 10. For the four-operational sensor case, the cost function has minimum value equal to 6.4 EU^2. With one of the umbrella sensor failed, the minimum value of J increased to 10.4 EU^2 at an umbrella angle of 15 deg. It is interesting to note that the cost function vs umbrella angle curve of case 2 remains relatively flat over a fairly large range of umbrella angles. This situation would allow for flexibility in the choice of instrument installation

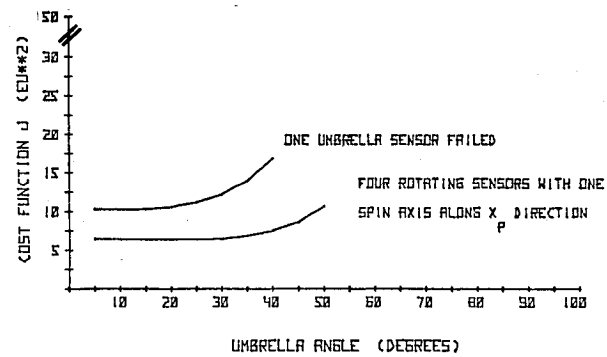

Fig. 10 Three spin axes in umbrella. Fourth spin axis along $\hat{x}_p$. Umbrella sensor spin axes symmetrically placed about $\hat{x}_p$ (120-deg intervals).

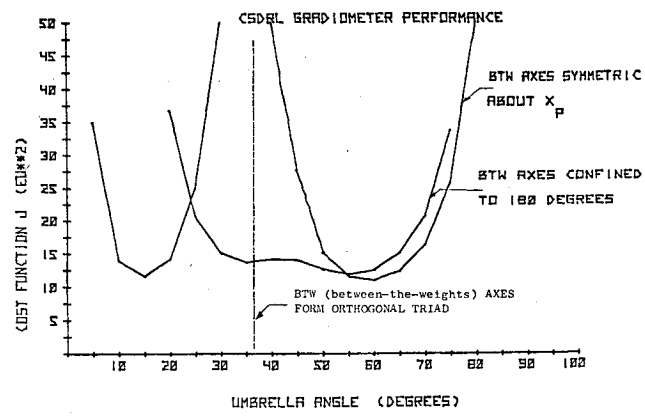

Fig. 11 Gradient measurement using three Draper Laboratory gradiometers.

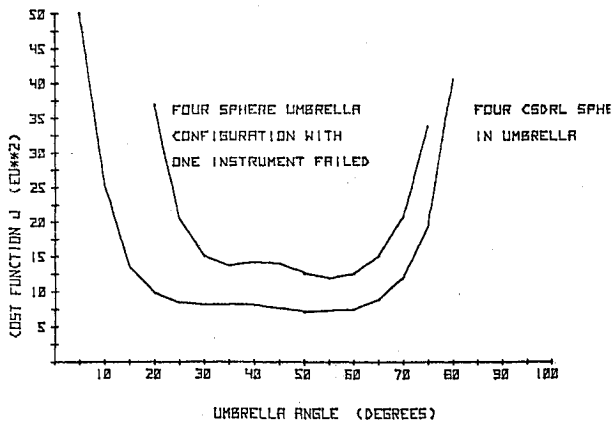

Fig. 12 Gradient estimation with four Draper Laboratory spherical sensors. All four BTW (between-the-weights) axes lie in the umbrella.

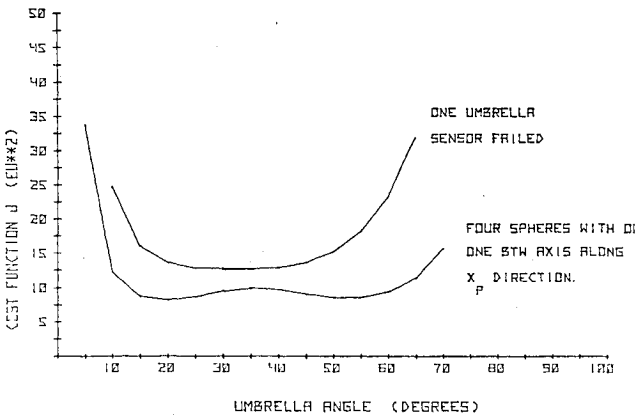

Fig. 13 Gradient estimation with four Draper Laboratory spherical sensors. One BTW axis lies along $\hat{x}_p$; other BTW axes symmetrically spaced about $\hat{x}_p$.

orientation without significant sacrifice of gradient determination accuracy. Accurate measurement of the spin axis alignment still is required, however.

VII. Measuring the Gravity Gradient Tensor with the Draper Laboratory Gravity Gradiometer

A similar performance analysis also was carried out for the Draper Laboratory spherical gradiometer system. For a triad composed of three spherical sensors, the defining equation has the form of Eq. (47). Matrix M of Eq. (47) is similar in nature to M' of Eq. (28) in that it is composed of products of Euler rotations. Note that the scalar multiplicative coefficient for this instrument is $2mr^2$, whereas it was $4mr^2$ for the Hughes' sensor:

$$\begin{bmatrix} A_{1\hat{i}} \\ A_{1\hat{j}} \\ A_{2\hat{i}} \\ A_{2\hat{j}} \\ A_{3\hat{i}} \\ A_{3\hat{j}} \\ 0 \end{bmatrix} = 2mr^2 \left[\begin{array}{c} \\ \\ M_{6\times 6} \\ \\ \\ \hline 1\ 1\ 1\ 0\ 0\ 0 \end{array}\right] \begin{bmatrix} \Gamma_{xx} \\ \Gamma_{yy} \\ \Gamma_{zz} \\ \Gamma_{xy} \\ \Gamma_{xz} \\ \Gamma_{yz} \end{bmatrix} \tag{47}$$

The analytical development of the gradient tensor estimate for this instrument system is similar to that of the Hughes' instrument and appears in Ref. 9. Optimal sensor orientation again is defined to be that which minimizes the cost function specified in Eq. (38). The results of the three-instrument analysis are shown in Fig. 11. For the Draper Laboratory sensor, the between-the-weights axis has essentially the same significance as the spin axis has for the rotating sensors. The $\hat{j}$ axis angular rotation β, is identical to the umbrella angles discussed in connection with the Hughes' sensor spin axis orientations.

The performance plots of Fig. 11 shows that the cost function J is minimized when the between-the-weights axes are located symmetrically about $\hat{x}_p$ and rotated out of the $\hat{y}_p - \hat{z}_p$ plane through an umbrella angle of approximately 58 deg. The value of J at that point was found to be approximately 10.8 EU^2. Note that, for the symmetric between-the-weights axes case, a singularity exists at an umbrella angle of 35.2644 deg. It is easy to show that a singularity always exists for this three-sensor system when the between-the-weights axes form an orthogonal triad.[9]

Four-sensor gradient tensor estimation also was considered for the Draper Laboratory sensor. The following cases were evaluated: 1) four sensors symmetrically located about $\hat{x}_p$ having identical umbrella angles β; and 2) a single sensor having its between-the-weights axis vertical (three sensors symmetrically located about $\hat{x}_p$ having identical umbrella angles β). The results of these tests for the four-sensor and one-sensor-failed cases are given in Figs. 12 and 13.

The cost function vs umbrella angle curve for the case where all four BTW (between-the-weights) axes are spaced symmetrically about $\hat{x}_p$ appears in Fig. 12. With four sensors operating, the minimum cost function occurred at an umbrella angle of 50 deg and had a value of 7.1 EU^2. With one sensor failed, the minimum value of the cost function increased to 11.9 EU^2 at 55 deg.

The effect of removing one of the BTW axes from the umbrella and placing it along $\hat{x}_p$ is shown in Fig. 13. For this case, the minimum value of J occurs at an umbrella angle of 20 deg and has value equal to 8.25 EU^2. At β equal to 55 deg, the value of J is 8.6 EU^2. With one umbrella sensor failed, the minimum value of the cost function was found to be 12.66 EU^2 at an umbrella angle of 35 deg.

VIII. Conclusions

The results presented in this paper show that three spinning gravity gradiometers will provide a gradient estimate having minimum error when the sensor spin axes form an orthogonal triad. A fourth gradiometer provides redundancy and prevents mission loss due to a single instrument failure. It has been shown that, with four spinning sensors, the best information is obtained with an umbrella configuration in which one sensor spin axis lies along $\hat{x}_p$, and the other spin axes are space symmetrically about $\hat{x}_p$. Changes as large as 5 deg, as long as they are well known for the instrument mounting, will not degrade the performance of the sensor system substantially. Furthermore, it is concluded that, for a spinning sensor system, an umbrella angle of 20 deg provides a reasonable compromise between four-sensor system optimal performance and performance degradation due to the loss of one sensor.

For the three static gradiometer system, it was found that BTW axis symmetry about $\hat{x}_p$ and an umbrella angle of approximately 58 deg minimized the cost function J. This result was in general agreement with those of Ref. 6. It also is concluded that a four-static gradiometer system should be configured with one BTW axis along $\hat{x}_p$ and the other located symmetrically about x_p with umbrella angles of 20 deg. The 20-deg umbrella angle selection is based on one-instrument-failure considerations.

Acknowledgment

This research was supported by Air Force Geophysics Laboratory Contract F19628-76-C-0109.

References

[1]Metzger, E.H. and Jircitano, A., "Inertial Navigation Performance Improvement Using Gravity Gradient Matching Techniques," AIAA Paper 75-1092, Boston, Mass., Aug. 1975, also *Journal of Spacecraft and Rockets*, Vol. 13, June 1976, pp. 323-324.

[2]Britting, K.R., Madden, S.J., and Hildebrandt, R.A., "Assessment of the Impact of Gradiometer Techniques on the Performance of Inertial Navigators," Air Force Cambridge Research Labs., Bedford, Mass., AFCRL-71-0465, Sept. 1971.

[3]Beyer, L.A., "Proposed Development of a Gravity Gradiometer for Energy Resource Exploration and Exploitation," U.S. Dept. of the Interior, Geological Survey Branch, Memo. to R.P. Sheldon, Menlo Park, Calif., Jan. 22, 1973.

[4]Ames, B.D., Forward, R.L., et al., "Prototype Moving Base Gravity Gradiometer," Hughes Research Labs., Malibu, Calif., R&D Design Evaluation Rept., Jan. 1973.

[5]Metzger, E.H. and Jircitano, A., "Analysis of Real Time Mapping of Horizontal and Vertical Gravity Anomalies Aboard a Moving Vehicle Such as an Aircraft," *International Symposium on Application of Marine Geodesy*, Columbus, Ohio, June 1974.

[6]Trageser, M.B., "A Gradiometer System for Gravity Anomaly Surveying," *Advances in Dynamic Gravimetry, Proceedings of the Symposium on Dynamic Gravimetry*, edited by T. Kattner, Fort Worth, Texas, March 1970.

[7]Trageser, M.B., "Feasibility Model Gravity Gradiometer Test Results," AIAA Paper 75-1093, Aug. 1975.

[8]Karamcheti, K., *Vector Analysis and Cartesian Tensors*, Holden-Day, Inc., San Francisco, Calif., 1967.

[9]DeBra, D.B. and Pelka, E.J., "Gravity Gradiometer Signal Detection, Parameter Identification, and On-line Parameter Control," Dept. of Aeronautics and Astronautics, Guidance and Control Lab., Stanford Univ., Stanford, Calif., AFGL Final Rept., Contract F 19628-75-C-0162, Dec. 1976.